

Excellence in Chemistry Research

Announcing our new flagship journal

- Gold Open Access
- Publishing charges waived
- Preprints welcome
- Edited by active scientists



Meet the Editors of *ChemistryEurope*



Luisa De Cola

Università degli Studi
di Milano Statale, Italy



Ive Hermans

University of
Wisconsin-Madison, USA



Ken Tanaka

Tokyo Institute of
Technology, Japan

Predictive TDDFT Methodology for Aromatic Molecules UV-Vis properties: from Benchmark to Applications

Matthieu Hédouin,^[a] Eleonora Luppi,^[b] Oliver Ward,^[c] David Harrowven,^[c] Catherine Fressigné,^{*[a]} and Isabelle Chataigner^{*[a, b]}

The absorption and emission properties of a series of 44 aromatic molecules have been investigated in Time Dependent Density Functional Theory (TDDFT) using different exchange-correlation functionals. Solvent effects have been included within linear response (LR) and state specific (SS) polarisable continuum model (PCM). The comparison with experimental UV-Vis data showed reasonable agreement for all the aromatic molecules when ω B97XD with SS-PCM is used. In particular, we

found an accurate linear correlation between experimental and theoretical results which is revealed in an equation for absorption and another equation for emission derived from a linear fitting between theoretical and experimental data. Through these linear equations we propose a simple, pragmatic and effective approach able to describe and predict the absorption and the emission of aromatic molecules with a reasonable computational cost.

Introduction

The search for new organic molecules with relevant optical properties has become increasingly important in recent years as their application in various light-energy utilizing systems continues to expand.^[1] The optical properties of these molecules arise from complex mechanisms and require an accurate representation of the absorption bands.^[2] Indeed, the experimental absorption spectra often reveal multiple bands resulting from different electronic transitions, with similar intensities.^[3-4] This observation is even more pronounced in molecules with electron-donor and electron-acceptor functionalization, or when hydrogen bonds are present, leading to modifications in the electronic structure.

In addition to absorption phenomena, emission phenomena are also an interesting electronic transition, both from a technological and an industrial point of view. Many classes of molecules are known to have strong fluorescence properties,

such as coumarins or quinolines, inspiring a huge effort on the design of new photovoltaic materials,^[5] and in the field of molecular imaging based around such core structures.^[6]

In this context, aromatic dyes are particularly promising.^[7] Their molecular structure is obviously one of the key factors controlling the properties of the resulting materials. When designing new and efficient fluorescent dyes/sensors, for example, the ability to access target molecules with a diverse array of functionality is a key consideration, both in terms of time and ease of synthesis. However, when the link between functionalization and the effect it has on optical properties is unclear, these factors become difficult to assess. In such circumstances, theoretical chemistry can provide a powerful tool for predicting the properties of dyes and guiding synthetic endeavours. Most of these compounds are characterized by rigid aromatic frameworks where the determination of excited state properties is strongly influenced by the calculation method used (size of the basis set, correlation and solvation model).

The Density Functional Theory (DFT) method is a popular technique for performing electronic structure calculations, as it offers advantages in respect of the computational cost and molecular size ratio, making it suitable for the analysis of a large number of organic compounds. The extension of DFT to the time-dependent domain (TDDFT) was proposed 30 years ago by Runge and Gross.^[8] The subsequent derivation of linear response TDDFT equations by Casida,^[9] ensured that it became a well-established and successful approach for calculating the excitation energies of organic molecules. The performance of linear response TDDFT depends on the approximation used for the exchange-correlation response kernel. Recently, the use of (range-separated) hybrid approximations was shown to improve the description of Rydberg and charge-transfer excitation energies.^[10] The effects of the solvent on excitation energies have been successfully included in TDDFT to rationalize experimental results.^[11] Different approaches have been proposed in literature: linear response (LR),^[12] state specific (SS),^[13]

[a] Dr. M. Hédouin, Dr. C. Fressigné, Prof. I. Chataigner
Normandie Université, UNIROUEN, CNRS, INSA Rouen, COBRA laboratory,
F-76000 Rouen
E-mail: catherine.fressigne@univ-rouen.fr
isabelle.chataigner@univ-rouen.fr
Homepage: <https://www.lab-cobra.fr/annuaire/fressigne-catherine/>
<https://www.lab-cobra.fr/annuaire/chataigner-isabelle/>

[b] Dr. E. Luppi, Prof. I. Chataigner
Laboratoire de Chimie Théorique
Sorbonne Université and CNRS
F-75005, Paris

[c] O. Ward, Prof. D. Harrowven
School of Chemistry
University of Southampton
Highfield, Southampton, SOBJ (UK)

Supporting information for this article is available on the WWW under <https://doi.org/10.1002/slct.202301943>

© 2023 The Authors. ChemistrySelect published by Wiley-VCH GmbH. This is an open access article under the terms of the Creative Commons Attribution Non-Commercial NoDerivs License, which permits use and distribution in any medium, provided the original work is properly cited, the use is non-commercial and no modifications or adaptations are made.

state specific with linear response correction (cLR),^[14] and vertical excitation model (VEM).^[15] The performance of these approaches has been investigated for different types of molecules.^[16] and it has been pointed out that in some cases there is a need to simultaneously account for both LR and SS effects.^[14,17]

Here, we calculated, the absorption and emission energies of a series of 44 aromatic molecules, in TDDFT using the solvation method developed by Improrata et al.,^[13] and compared them to the experimental data. The excitation energies of the selected organic dyes were obtained using various functionals for the exchange-correlation kernel and linear-responses versus state-specific PCM have been investigated. From this analysis we show an excellent linear fit between calculated and experimental data. Even if the method does not include explicitly vibration and temperature effects,^[18] the linear correlation is reflected in two equations that fit linearly the absorption and emission results of aromatic molecules, at a reasonable computational cost.

Results and Discussion

We began our investigation with a series of fluorene based electroluminescent materials.^[19] Their emission properties are tuneable by altering the substitution pattern present.^[20] Assuming that the most important UV-Vis properties come from the aromatic core of the fluorene molecule, we first performed a Natural Transition Orbital (NTO) analysis for the electronic transitions of the molecule used experimentally, **1a full**, and the simplified model **1a** containing only the fluorene core (Figure 1).^[21] The dominant "Particle" \rightarrow "Hole" contributions and the associated weights for the first excitation ($S_0 \rightarrow S_1$) for the model fluorene are illustrated in Figure 1. The S_1 state, which determines the absorbance properties, revealed that the highest occupied natural transition orbital (HONTO) and the lowest unoccupied natural transition orbital (LUNTO) are mainly located at the core ring, which confirmed our hypothesis. This result allowed us to simplify the fluorene molecules studied as

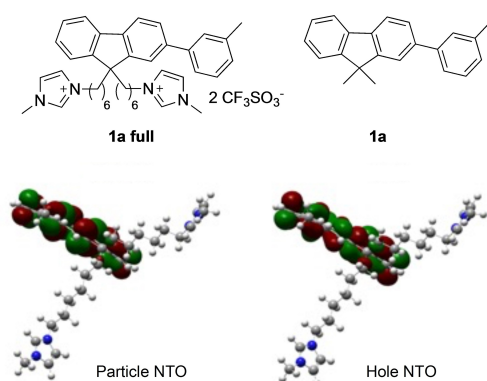


Figure 1. Structure of the experimentally used molecule **1a full** (up, left) and the simplified model **1a** (up, right) and calculated natural transition orbitals (NTOs) of the **1a full** (optimized geometry for the excited molecule without counter-ion) in acetonitrile.

the aromatic core alone could be used for the calculations (Figure 1, right).

The absorption properties of the model molecule **1a** in acetonitrile were investigated by TDDFT with linear response solvation and different functionals (see Supporting Information (SI), Table S1) containing Grimme's dispersion corrections and long-range correction for the Coulomb potential.^[22]

As shown in Figure 2 (blue sticks), the calculated absolute error of the absorption wavelength with respect to the extracted maximum experimental value indicate that the absorption properties are well reproduced by the functionals ω B97, ω B97X and ω B97XD. The absolute error increased with hybrid functionals like M062X or CAM-B3LYP, with a maximum with BLYP-D which is not corrected for the long-range Coulomb interaction.

Besides the accuracy of the exchange-correlation functionals used, the precision of the computational method to predict the excited state geometries and the optical properties is also limited by the description of the solvent. Nevertheless, to do so requires consideration of the solvation dynamics in the excited state. To that end, we compared the vertical excitations describe before using the linear response solvation (Figure 2, blue stick), with the state-specific solvation (Figure 3 orange stick, See also SI, Table S1).^[23] State-specific solvation is based on an external iteration approach, chosen to save and store the ground state solvation and transpose it unchanged to the excited state geometry. As shown in Figure 2 (orange sticks), the approach led to more accurate results, with a significant decrease in the absolute error of absorption $\lambda_{\text{calc}}^{\text{abs}}$ for all functionals. Notably, among the functionals that were already well performing in linear-response PCM, i.e. ω B97, ω B97X and ω B97XD, we found that, in state-specific PCM, the functional ω B97XD had a good performance. For the rest of our study, we thus decided to use ω B97XD because it gives more flexibility using different PCM approaches.

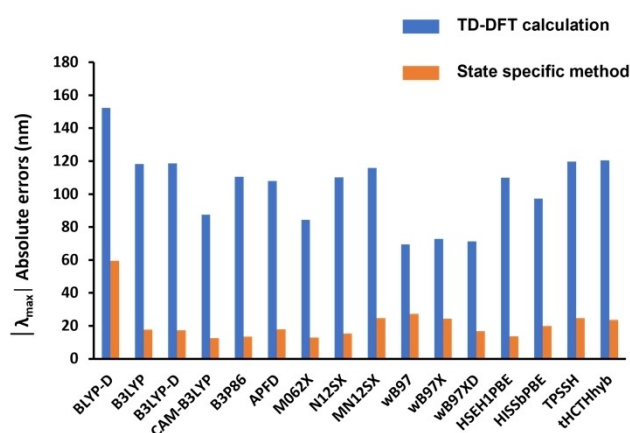
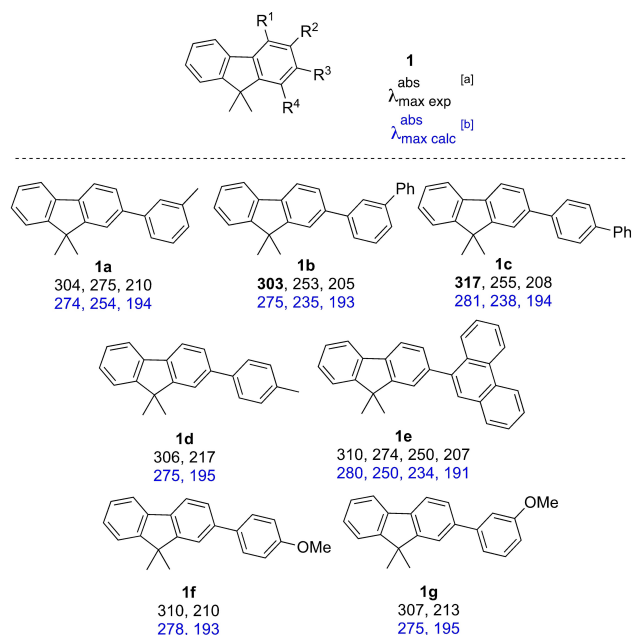


Figure 2. Absolute errors between the calculated maximum absorption wavelengths values and the experimental values for molecule **1a**, with the



[a] Experimental absorption wavelengths values ($\lambda_{\max}^{\text{exp}}$), in nm, extracted from UV-Vis spectra deconvolution (See SI, Fig 1S to 13S).
[b] Calculated absorption wavelengths values ($\lambda_{\max}^{\text{calc}}$), in nm.

Figure 3. comparison of the calculated (ω B97XD/6-31 + G**) and experimental $\lambda_{\max}^{\text{abs}}$ of model fluorene molecules.

Absorption properties

The absorptions of different substituted fluorene molecules were investigated using the state-specific method. In Figure 3, the experimental ($\lambda_{\text{exp}}^{\text{abs}}$) and calculated ($\lambda_{\text{calc}}^{\text{abs}}$) absorptions for 13 model molecules are presented (for complete data, see SI, Table S2). They revealed an underestimation of the calculated $\lambda_{\text{calc}}^{\text{abs}}$ absorption values. Notably, a quasi-systematic and reproducible underestimation of the calculated data was observed, with a good linear correlation ($R^2 = 0.991$, Figure 4).

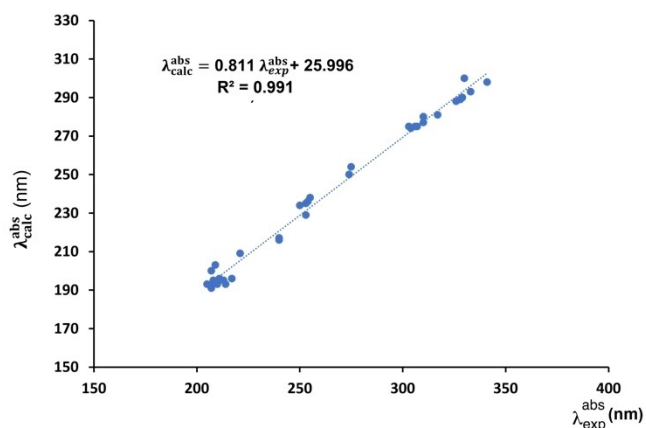
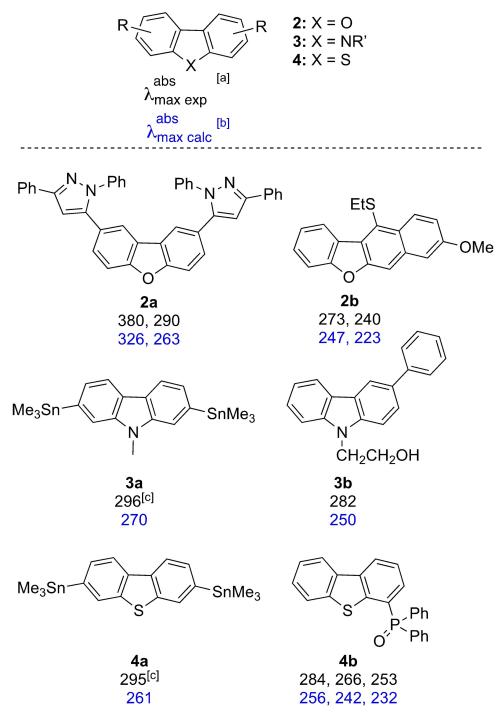


Figure 4. Graphical correlation between the experimental and the calculated absorption $\lambda_{\max}^{\text{abs}}$, obtained by ω B97XD/6-31 + G** state specific method, for the fluorene molecules

The electronic transition exhibits a clear $\pi \rightarrow \pi^*$ character, with oscillator strength up to 0.5. Substitution at one side of the molecules (molecules 1a–g) led to more energetic absorptions, with experimental $\lambda_{\max}^{\text{exp}}$ values between 303 and 317 nm. On the other hand, substitution on both sides of the fluorene core (molecules 1h–m, see SI) led to less energetic transitions, with experimental $\lambda_{\text{exp}}^{\text{abs}}$ absorptions between 326 and 341 nm.

To study the performance of this methodology, its extension to new aromatic derivatives was undertaken with some dibenzofuranic (2a–c), carbazolic (3a–c) and dibenzothiophenic (4a–c) compounds. These compounds differed from the fluorenes through substitution of the central carbon atom by a heteroatom, thereby extending the aromatic ring system. In Figure 5, $\lambda_{\text{exp}}^{\text{abs}}$ and $\lambda_{\text{calc}}^{\text{abs}}$ are reported (For complete data, see SI, Table S2). For some of these molecules, each being characterized by an increase of the experimental $\lambda_{\text{exp}}^{\text{abs}}$ range. Adding these results to those reported in Figure 4, we still find a very good linear correlation with the experimental data ($R^2 = 0.988$).

For these compounds, more energetic theoretical transitions were observed, between 223 and 270 nm, except for the molecule 2a (326 nm). The presence of a heteroatom in the aromatic core is handled well by our method. A correlation between the decrease in λ_{\max} absorption and the electro-negativity of the central atom is noteworthy. Substitution by a methylene led to calculated λ_{\max} values of 303 and 341 nm,



[a] Experimental absorption wavelengths values, $\lambda_{\text{exp}}^{\text{abs}}$, in nm, extracted from literature data (see SI). [b] Calculated absorption wavelengths values, $\lambda_{\max}^{\text{calc}}$, in nm. [c] With Si atoms in replacement of Sn atoms for functional consideration

Figure 5. Comparison of the calculated (ω B97XD/6-31 + G**) and experimental $\lambda_{\max}^{\text{abs}}$ of some dibenzofuranic, dibenzocarbazolic and dibenzothiophenic molecules.

while its replacement by a nitrogen atom led to values between 250 and 270 nm, going to 223 and 263 nm with an oxygen atom. However, this observation is only valid for elements within the same period.

We then considered molecules with less extended aromatic ring systems *e.g.* indoles **5**; more extended aromatic ring systems *e.g.* anthracenes **6**, and divinylarenes *e.g.* **7**. Some of these derivatives are listed in Figure 6 (for complete data, see SI, Table S2) with their experimental and calculated λ_{\max} absorptions all showing a good correlation between these data. As with the previous observations, the indole derivatives led to more energetic absorption transitions, with calculated λ_{\max} values between 196 and 285 nm. Extending the aromatic ring system to anthracene or linking them by alkene conjugation leads to an increase in the calculated λ_{\max} in accordance with the experimental data. Coumarins **8**, phenanthrenes **9** and anthracene-9,10-dione derivatives **10** were also considered. Some of these compounds are listed in Figure 6 together with the experimental and calculated $\lambda_{\max}^{\text{abs}}$ values (for complete data, see SI, Table S2). As shown in Figure 6, phenanthrenes and anthracene-9,10-diones exhibit less ener-

getic transitions than the other molecules, between 253 and 428 nm, in accordance with the experimental data. The incorporation of these compounds facilitates an increase in the λ_{\max} absorption, with an experimental range between 205 and 500 nm. The linear correlation ($R^2=0.991$) remains quite good considering the diversity of these molecules and the range of absorption wavelengths (Figure 7).

This TDDFT with ω B97XD/6-31+G** with state specific PCM demonstrated to be a quite accurate strategy to describe a large variety of molecular systems and wavelengths. The correlation we found between calculated and experimental data permitted us to accurately fit the data in a linear equation which can then be used to predict the absorption properties of a vast array of aromatic compounds.

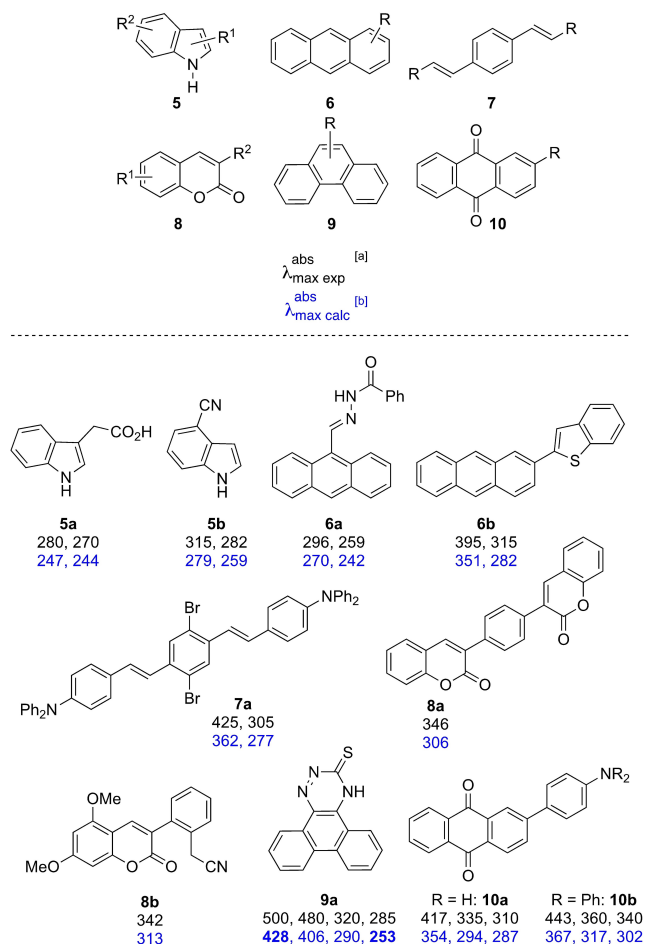
Emission properties

The emission properties for these aromatic molecules were also considered. The calculated $\lambda_{\max}^{\text{em}}$ emissions were determined by the state specific method with ω B97XD. In Figure 8, the experimental and calculated data are listed and compared. The electronic transition exhibits a clear $\pi \rightarrow \pi^*$ character, with oscillator strength up to 0.5.

As shown with the absorption properties, our approach correctly represents the emission process, and gave a good prediction of the $\lambda_{\text{exp,abs}}^{\text{em}}$ for the fluorene molecules. In Figure 9, we show that the data fit between calculated and experimental data for emission with these molecules has a good linear regression ($R^2=0.990$).

The structures considered above for the absorption properties were also investigated for the emission process. As with the absorption properties, a good prediction of the emission process was observed for these aromatic compounds, as evidenced by the excellent linear correlation ($R^2=0.994$, Figure 10).

Expectedly, compounds with the less energetic absorption transitions (anthracene-9,10-diones **9** and phenanthrenes **10**) also gave less energetic emission values, in the range of 450 to 730 nm. Dibenzofurans **2**, dibenzothiophenes **4** and indoles **5**



[a] Experimental wavelengths values, $\lambda_{\max}^{\text{abs exp}}$, in nm, from literature data (see SI). [b] Calculated wavelengths values, $\lambda_{\max}^{\text{abs calc}}$, in nm.

Figure 6. Analysis of the calculated (ω B97XD/6-31+G**) and experimental

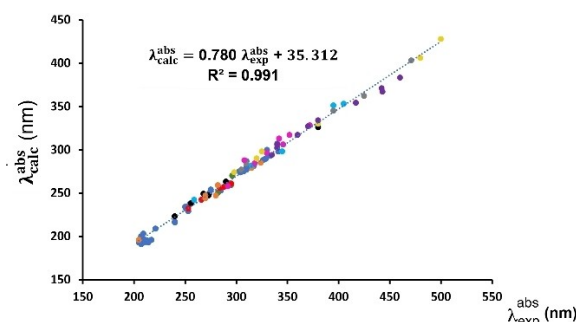
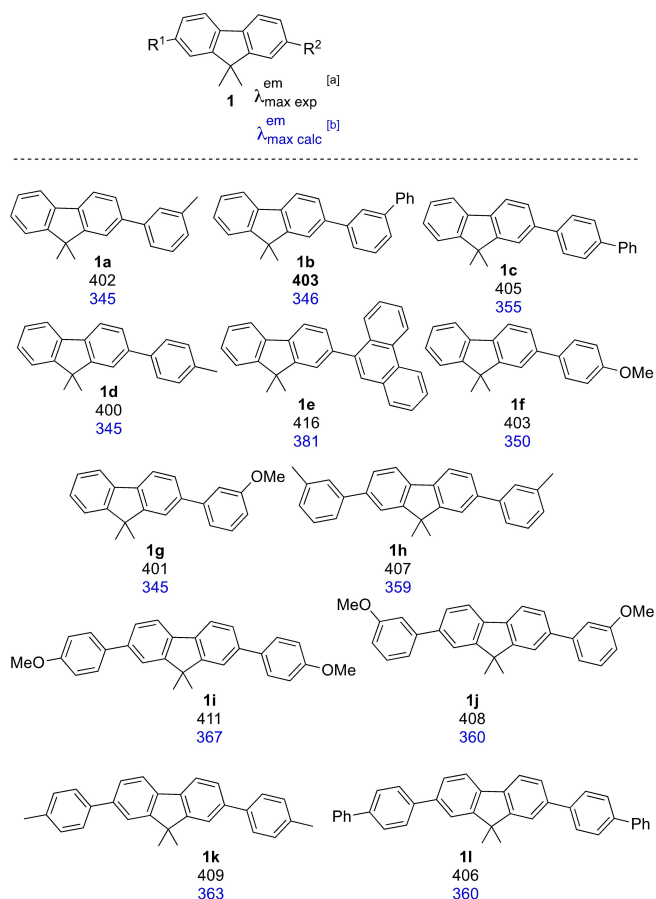


Figure 7. Graphical correlation between the experimental and the calculated absorption λ_{\max} , obtained by ω B97XD/6-31+G** state specific method, for the fluorenes (in blue), dibenzothiophenes (in red), dibenzofurans (in black), carbazoles (in green), indoles (in orange), anthracenes (in light blue), benzenes (in grey), coumarins (in pink), phenanthrenes (in light green) and anthracene-9,10-diones (in purple).



[a] Experimental $\lambda_{\max}^{\text{em exp}}$ values, in nm, from UV-Vis spectra deconvolution (See SI, Fig S1 to S13). [b] Calculated $\lambda_{\max}^{\text{em calc}}$, in nm.

Figure 8. Analysis of the calculated (ω B97XD/6-31 + G**) and experimental emission $\lambda_{\max}^{\text{em}}$ of fluorene molecules

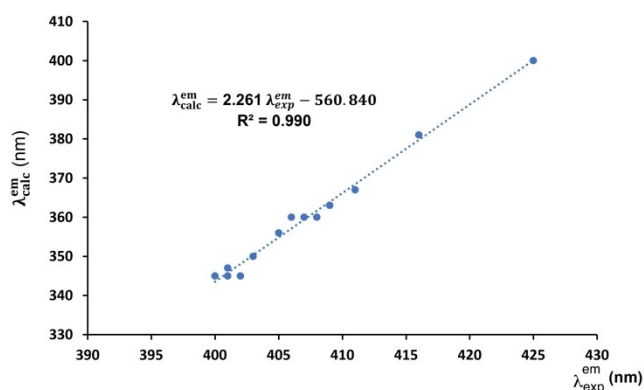


Figure 9. Graphic correlation between the experimental and the calculated emission $\lambda_{\max}^{\text{em}}$, obtained by ω B97XD/6-31 + G** state specific method, for the fluorene molecules

gave more energetic emission values. Notably, their range of experimental $\lambda_{\text{exp}}^{\text{em}}$ spans in a range from 337 nm (UV-A) to 695 nm (red light).

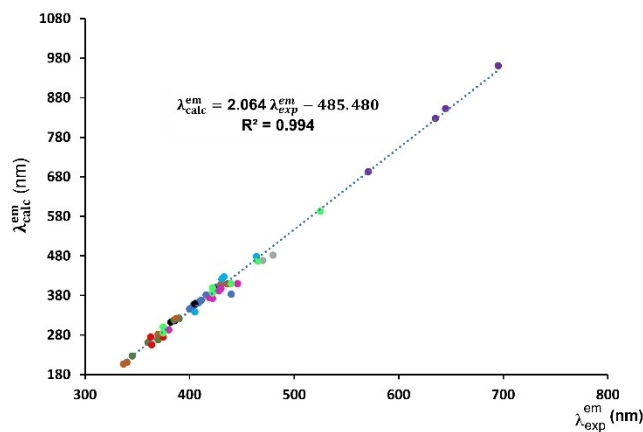


Figure 10. Graphical correlation between the experimental and the calculated emission $\lambda_{\max}^{\text{em}}$, obtained by ω B97XD/6-31 + G** state specific method, for the fluorenes (in blue), dibenzothiophenes (in red), dibenzofurans (in black), carbazoles (in green), indoles (in orange), anthracenes (in light blue), benzenes (in grey), coumarins (in pink), phenanthrenes (in light green) and anthracene-9,10-diones (in purple).

The study of calculated vs experimental emission proved that, as with absorption, the data can be fitted in a linear equation covering a wide wavelength emission range. Therefore, this fit is a valuable tool for the design of new aromatic organic dyes with specific emission characteristics.

Theoretical prediction of absorption and emission of a new molecule

The previous investigations on absorption and emission brought us to obtain the two linear equations, from which, once $\lambda_{\text{calc}}^{\text{abs}}$ and $\lambda_{\text{calc}}^{\text{em}}$ have been calculated it is possible to accurately predict the experimental values $\lambda_{\text{exp}}^{\text{abs}}$ and $\lambda_{\text{exp}}^{\text{em}}$.

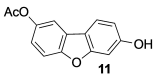
$$\lambda_{\text{pred}}^{\text{abs}} = (\lambda_{\text{calc}}^{\text{abs}} - 35.312)/0.780 \quad (1)$$

$$\lambda_{\text{pred}}^{\text{em}} = (\lambda_{\text{calc}}^{\text{em}} + 485.480)/2.064 \quad (2)$$

In order to evaluate our method, and therefore verify the reliability of the predicted $\lambda_{\text{exp}}^{\text{abs}}$ and $\lambda_{\text{exp}}^{\text{em}}$, we calculated the optical properties of the dibenzofuran derivative **11** whose structure is shown in Table 1. We obtained 4 major transitions (oscillator strength more important than 0.2) in the UV-Vis range. The results are reported in Table 1. Then, we used Eq. (1) and (2) to predict the expected experimental values $\lambda_{\text{pred}}^{\text{abs}}$ and $\lambda_{\text{pred}}^{\text{em}}$, as reported in Table 1.

Next, compound **11** was synthesized by the reaction between 5-acetoxy-3-nitrobenzofuran and the Danishefsky diene, followed by re-aromatization on heating.^[24] The synthetic sample exhibited four $\lambda_{\text{exp}}^{\text{abs}}$ and four $\lambda_{\text{exp}}^{\text{em}}$ maxima, which are listed and compared in Table 1. The precision of the state-specific method without correction gave values with errors ranging from 7.1 to 17.3% in absorption and from 24.0 to 60.0% in emission (see SI, Table S3). After correction with the

Table 1. Comparison of the predicted (ω B97XD/6-31 + G**) and experimental absorption and emission wavelengths of molecule 11.

Entry				
	$\lambda_{\max \text{ exp}}^{\text{abs}}$ (nm) ^[a]	$\lambda_{\text{ pred}}^{\text{abs}}$ (nm)	$\lambda_{\max \text{ exp}}^{\text{em}}$ (nm) ^[a]	$\lambda_{\text{ pred}}^{\text{em}}$ (nm)
1	308	292	366	379
2	296	283	346	343
3	256	246	331	332
4	227	226	320	331

[a] Absorption and emission wavelengths values, in nm, extracted from UV-Vis spectra deconvolution (See SI).

predictive equation, the errors decreased to 0.6–5.6% in absorption and 0.9–3.5% for emission.

Limits of the theoretical predictions

We also investigated the possibility of expanding our predictive approach to conjugated alkenes. As a model, we chose one of the most important and common dyes, β -carotene, in its linear conformation (for structure optimization, see SI, Structure data section). The state-specific methodology was employed to determine the calculated UV-Vis properties of this compound. The corresponding absorption and emission values are listed in Table 2. The calculated absorption and emission values showed much larger relative errors when compared to the experimental data, up to 13%, making it too large to integrate these species within the same model. This demonstrates that our approach works for aromatic systems but does not extend to conjugated alkenes which require the development of a different model.

Conclusions

In conclusion, an investigation into the optical absorptions and emissions of aromatic dyes with TDDFT/PCM and a state specific method was undertaken. Of the many functionals investigated we found ω B97XD to be highly efficient for predicting both their absorption and emission spectra over a wide spectral range. The state specific method permitted the accurate incorporation of solvent effects in the description of the vertical excitation energies as well as the ground and excited relaxation steps. The good correlation achieved

Table 2. Comparison of the calculated (ω B97XD/6-31 + G**) and experimental wavelength absorption values of β -carotene.

Entry	$\lambda_{\max \text{ exp}}^{\text{abs}}$ (nm) ^[a]	$\lambda_{\max \text{ calc}}^{\text{abs}}$ (nm)	$\lambda_{\max \text{ exp}}^{\text{em}}$ (nm) ^[a]	$\lambda_{\max \text{ calc}}^{\text{em}}$ (nm)
	β -carotene	452.4	507.3	570.0
(linear conformation)	401.2	362.1		
	283.0	300.6		
	264.5	268.1		

[a] Absorption maxima value extracted from literature data (See SI).

between the calculated and experimental data led us to extract a linear correlation allowing for the prediction of UV-Vis properties of a diverse array of small aromatic molecules by correction of the “raw” calculated data. These equations are obtained from theoretical calculations which do not include explicitly vibrations and temperature effects. However, these effects are self-contained in the coefficients of the fitting. This approach is simple, pragmatic, effective and computationally profitable to predict the optical properties of a large variety of aromatic compounds. Of the systems studied, only conjugated polyalkenes proved intractable using this model. The method was successfully used to predict the UV-Vis properties of a molecule prior to its synthesis and evaluation. The excellent correlation between the experimental data and the predicted corrected wavelengths, for both absorption and emission, highlights the relevance of our predictive model.

In the future, it will be interesting to investigate if the linear correlation is still present for the 0–0 energies, extracting these energies from experiments and calculating them in TDDFT/SS-PCM with ω B97XD.^[25] Furthermore, more insight in the correlation can be given by a further analysis with other methods for solvents such as cLR and VEM. An obvious next step is the extension of this methodology to larger aromatic systems, and those containing metals, which will be undertaken in the near future.

Computational methods

For this study DFT and TDDFT with PCM have been used. The hybrid functional ω B97XD combined with the 6-31 + G(d,p) basis set provide an adequate description of the geometries and excitations in both ground- and excited states for the different molecules. The ground- and excited-state geometries of each molecule have been fully optimised without any symmetry restriction. The ground-state geometry optimisations are repeated for all conformers of the molecules, and the corresponding excited state calculations arise from the most stable conformer. Following each optimisation in the ground or in the excited state, the harmonic frequencies have been computed and systematically checked in order to confirm that all vibrational frequencies are real and not imaginary, to correspond to minima.

TDDFT methodology was used to investigate the excited states of interest. In accordance with the geometry optimization, the ω B97XD/6-31 + G(d,p) level was chosen. The lowest 20 singlet-singlet vertical electronic excitations were calculated, and only the major ones were chosen (oscillator strength up to 0.1). The geometry of the lowest singlet excited state of each compound was relaxed using TDDFT, followed by harmonic frequencies calculations to verify the presence of a minimum.

The state-specific method was used in order to take into account the solvent effect described by PCM. For the absorption, the molecule was optimised in its ground-state and the information about solvation were stored. Then the vertical excitation was calculated using the solvation previously stored in a non-equilibrium calculation. In the case of emission, the molecule was optimised in its excited-state and also in this

case the information about solvation was stored. Then the ground-state energy at this geometry, with the non-equilibrium solvation stored previously was calculated. The difference between the energies in the excited and ground state give the vertical emission energy.

TDDFT calculations were performed using 16 functionals : GGA with dispersion model (BLYP-D),^[26] hybrid functionals (B3LYP,^[27] B3LYP-D,^[16] B3P86,^[28] APFD,^[29] M062X,^[30] N12SX,^[31] MN12SX,^[20] HSEH1PBE^[32] and HISSbPBE),^[33] hybrid functionals with τ -dependent gradient corrected (TPSSH^[34] and tHCTHhyb)^[35] and Long-Range corrected functionals (CAM-B3LYP,^[36] ω B97, ω B97X and ω B97XD).³⁷ ω B97XD/6-31+G(d,p) was then selected as the most appropriate method.

All calculations were performed using the Gaussian16 software and the models of electron density of various energy levels were visualized on GaussView version 6.1.

Supporting Information Summary

Supporting information section describes the computed cartesian coordinates for all compounds (Ground state, Excited state and Excited state, relaxed), Tables S1–S3^[38] and Figures S1–S14 (Experimental absorption and emission of fluorene molecules 1a–1m and 11).

Acknowledgements

The authors acknowledge the European France- (Manche)-England cross-border cooperation program INTERREG V A (Project 208, "SmartT"), co-financed by ERDF, for financial support. This work has been partially supported by University of Rouen Normandy, the CNRS, INSA Rouen, European Regional Development Fund (ERDF), Labex SynOrg (ANR-11-LABX-0029), Carnot Institute I2C, the graduate school for research XI-Chem (ANR-18-EURE-0020 XL-CHEM), and by Region Normandie. CRIANN is also acknowledged for their allocation of computer time.

Conflict of Interests

The authors declare no conflict of interest.

Data Availability Statement

The data that support the findings of this study are available in the supplementary material of this article.

Keywords: Correction term · Excited States · Quantum chemical calculation · Time-dependent density functional theory · UV/Vis spectroscopy

- [1] a) A. Hagfeldt, G. Boschloo, L. Sun, L. Kloo, H. Pettersson, *Chem. Rev.* **2010**, *110*, 6595–6663; b) X. Chen, T. Pradhan, F. Wang, J. S. Kim, J. Yoon, *Chem. Rev.* **2011**, *112*, 1910–1956; c) L. D. Lavis, *Annu. Rev. Biochem.* **2017**, *86*, 825–843; d) L. Wang, M. S. Frei, A. Salim, K. Johnsson, *J. Am. Chem. Soc.* **2018**, *141*, 2770–2781; e) A. Nina-Diogo, B. Bertrand, S. Thorimbert, G. Gontard, S. Nasseem-Kahn, A. Echeverri, J. Contreras-

- García, C. Allain, G. Lemerrier, E. Luppi, C. Botuha, *Adv. Opt. Mater.* **2023**, 2300336.
- [2] a) M. Klessinger, J. Michl, *Excited states and photochemistry of organic molecules*, VCH, **1995**, 1–135; b) T. Le Bahers, T. Pauporté, G. Scalmani, C. Adamo, I. Ciofini, *Phys. Chem. Chem. Phys.* **2009**, *11*, 11276; c) A. D. Laurent, C. Adamo, D. Jacquemin, *Phys. Chem. Chem. Phys.* **2014**, *16*, 14334–14356; d) A. V. Kulinich, N. A. Derevyanko, A. A. Ishchenko, N. B. Gussyak, I. M. Kobasa, P. P. Romańczyk, S. S. Kurek, *Dyes Pigm.* **2019**, *161*, 24–33; e) F. A. AL-Temimeh, A. H. Omran Alkhayatt, *Optik* **2020**, *208*, 163920.
- [3] a) H. Zollinger, *Color chemistry : syntheses, properties and applications of organic dyes and pigments*, John Wiley & Sons, **2003**, 20–45; b) C.-R. Zhang, Z.-J. Liu, Y.-H. Chen, H.-S. Chen, Y.-Z. Wu, W. Feng, D.-B. Wang, *Curr. Appl. Phys.* **2010**, *10*, 77–83; c) R. El-Shishtawy, S. Elroby, A. Asiri, K. Müllen, *Int. J. Mol. Sci.* **2016**, *17*, 487; d) A. B. El-Meligy, N. Koga, S. Iuchi, K. Yoshida, K. Hirao, A. H. Mangood, A. M. El-Nahas, *J. Photochem. Photobiol. A* **2018**, *367*, 332–346.
- [4] a) B. Mennucci, *WIREs Comput. Mol. Sci.* **2012**, *2*, 386–404; b) A. Charaf-Eddin, A. Planchat, B. Mennucci, C. Adamo, D. Jacquemin, *J. Chem. Theory Comput.* **2013**, *9*, 2749–2760; c) Y. Wang, L. Cai, W. Chen, D. Wang, S. Xu, L. Wang, M. A. Kononov, S. Ji, M. Xian, *Chem. Methods* **2021**, *1*, 389–396; d) G. C. Santos, J. C. Roldao, J. Shi, B. Milián-Medina, L. C. Silva-Filho, J. Gierschner, *ChemPhysChem* **2020**, *21*, 1797–1804.
- [5] R. M. Christie, *Colour Chemistry*, Royal Society of Chemistry, **2015**.
- [6] a) H. Zollinger, *Color chemistry : syntheses, properties and applications of organic dyes and pigments*, John Wiley & Sons, **2003**, 20–45; b) C.-R. Zhang, Z.-J. Liu, Y.-H. Chen, H.-S. Chen, Y.-Z. Wu, W. Feng, D.-B. Wang, *Curr. Appl. Phys.* **2010**, *10*, 77–83; c) R. El-Shishtawy, S. Elroby, A. Asiri, K. Müllen, *Int. J. Mol. Sci.* **2016**, *17*, 487; d) A. B. El-Meligy, N. Koga, S. Iuchi, K. Yoshida, K. Hirao, A. H. Mangood, A. M. El-Nahas, *J. Photochem. Photobiol. A* **2018**, *367*, 332–346.
- [7] K. L. Do, M. Su, F. Zhao, *Dyes Pigm.* **2022**, *205*, 110482.
- [8] E. Runge, E. K. U. Gross, *Phys. Rev. Lett.* **1984**, *52*, 997–1000.
- [9] M. E. Casida, *Recent Advances in Density Functional Methods*, WORD SCIENTIFIC **1995**, 155–192.
- [10] J. Toulouse, *ArXiv* **2021**, DOI 10.48550/ARXIV.2103.02645.
- [11] a) B. Mennucci, *WIREs Comput. Mol. Sci.* **2012**, *2*, 386–404; b) A. Charaf-Eddin, A. Planchat, B. Mennucci, C. Adamo, D. Jacquemin, *J. Chem. Theory Comput.* **2013**, *9*, 2749–2760; c) Y. Wang, L. Cai, W. Chen, D. Wang, S. Xu, L. Wang, M. A. Kononov, S. Ji, M. Xian, *Chem. Methods* **2021**, *1*, 389–396; d) G. C. Santos, J. C. Roldao, J. Shi, B. Milián-Medina, L. C. Silva-Filho, J. Gierschner, *ChemPhysChem* **2020**, *21*, 1797–1804.
- [12] R. Cammi, B. Mennucci, *J. Chem. Phys.* **1999**, *110*, 9877–9886.
- [13] a) R. Improta, V. Barone, G. Scalmani, M. J. Frisch, *J. Chem. Phys.* **2006**, *125*, 054103; b) R. Improta, G. Scalmani, M. J. Frisch, V. Barone, *J. Chem. Phys.* **2007**, *127*, 074504; c) P. Zhou, M. R. Hoffmann, K. Han, G. He, *J. Phys. Chem. B* **2014**, *119*, 2125–2131.
- [14] M. Caricato, B. Mennucci, J. Tomasi, F. Ingrosso, R. Cammi, S. Corni, G. Scalmani, *J. Chem. Phys.* **2006**, *124*, 124520.
- [15] a) J. Li, C. J. Cramer, D. G. Truhlar, *Int. J. Quantum Chem.* **2000**, *77*, 264–280; b) A. V. Marenich, C. J. Cramer, D. G. Truhlar, C. A. Guido, B. Mennucci, G. Scalmani, M. J. Frisch, *Chem. Sci.* **2011**, *2*, 2143.
- [16] a) C. A. Guido, G. Scalmani, B. Mennucci, D. Jacquemin, *J. Chem. Phys.* **2017**, *146*, 204106; b) C. Katan, P. Savel, B. M. Wong, T. Roisnel, V. Dorcet, J.-L. Fillaut, D. Jacquemin, *Phys. Chem. Chem. Phys.* **2014**, *16*, 9064–9073; c) X. Blase, I. Duchemin, D. Jacquemin, *Chem. Soc. Rev.* **2018**, *47*, 1022–1043.
- [17] J.-M. Mewes, J. M. Herbert, A. Dreuw, *Phys. Chem. Chem. Phys.* **2017**, *19*, 1644–1654.
- [18] a) M. Dierksen, S. Grimme, *J. Phys. Chem. A* **2004**, *108*, 10225–10237; b) F. Santoro, R. Improta, A. Lami, J. Bloino, V. Barone, *J. Chem. Phys.* **2007**, *126*, 084509; c) D. Jacquemin, E. Brémond, A. Planchat, I. Ciofini, C. Adamo, *J. Chem. Theory Comput.* **2011**, *7*, 1882–1892; d) E. Stendardo, F. Avila Ferrer, F. Santoro, R. Improta, *J. Chem. Theory Comput.* **2012**, *8*, 4483–4493; e) J. Cerezo, F. Santoro, *J. Chem. Theory Comput.* **2016**, *12*, 4970–4985; f) F. Muniz-Miranda, A. Pedone, G. Battistelli, M. Montalti, J. Bloino, V. Barone, *J. Chem. Theory Comput.* **2015**, *11*, 5371–5384; g) D. Aranda, F. Santoro, *J. Chem. Theory Comput.* **2021**, *17*, 1691–1700.
- [19] a) A. Yella, R. Humphry-Baker, B. F. E. Curchod, N. Ashari Astani, J. Teuscher, L. E. Polander, S. Mathew, J.-E. Moser, I. Tavernelli, U. Rothlisberger, M. Grätzel, Md. K. Nazeeruddin, J. Frey, *Chem. Mater.*

- 2013, 25, 2733–2739; b) K. R. Justin Thomas, A. Venkateswararao, V. Joseph, S. Kumar, J.-H. Jou, *Org. Electron.* **2019**, 64, 266–273; c) S. Arumugam, Y. Li, J. E. Pearce, K. L. Court, G. Piana, E. H. Jackman, O. J. Ward, M. D. B. Charlton, J. Tudor, D. C. Harrowven, S. P. Beeby, *Org. Electron.* **2022**, 105, 106513.
- [20] a) L. Ying, C.-L. Ho, H. Wu, Y. Cao, W.-Y. Wong, *Adv. Mater.* **2014**, 26, 2459–2473; b) J. Shaya, F. Fontaine-Vive, B. Y. Michel, A. Burger, *Chem. Eur. J.* **2016**, 22, 10627–10637; c) N. Xiang, Z. Gao, G. Tian, Y. Chen, W. Liang, J. Huang, Q. Dong, W.-Y. Wong, J. Su, *Dyes Pigm.* **2017**, 137, 36–42; d) F. Huo, H. Zhang, Z. Chen, L. Qiu, J. Liu, S. Bo, I. V. Kityk, *J. Mater. Sci. Mater. Electron.* **2019**, 30, 12180–12185.
- [21] a) E. Badaeva, V. V. Albert, S. Kilina, A. Kopolov, M. Sykora, S. Tretiak, *Phys. Chem. Chem. Phys.* **2010**, 12, 8902–8913; b) Y. Y. Pan, J. Huang, Z. M. Wang, S. T. Zhang, D. W. Yu, B. Yang, Y. G. Ma, *RSC Adv.* **2016**, 6, 108404–108410; c) P. Zhou, C. Ning, A. Alsaedi, K. Han, *ChemPhysChem* **2016**, 17, 3139–3145; d) H. Lim, H. J. Cheon, S. Woo, S. Kwon, Y. Kim, J. Kim, *Adv. Mater.* **2020**, 32, 2004083.
- [22] a) M. A. Rohrdanz, J. M. Herbert, *J. Chem. Phys.* **2008**, 129, 034107; b) J.-W. Song, M. A. Watson, A. Nakata, K. Hirao, *J. Chem. Phys.* **2008**, 129, 184113; c) B. M. Wong, J. G. Cordaro, *J. Chem. Phys.* **2008**, 129, 214703; d) K. Hirao, B. Chan, J.-W. Song, H.-S. Bae, *J. Phys. Chem. A* **2020**, 124, 8079–8087; e) T. Tsuneda, K. Hirao, *WIREs Comput. Mol. Sci.* **2014**, 4, 375–390.
- [23] a) R. Improta, V. Barone, G. Scalmani, M. J. Frisch, *J. Chem. Phys.* **2006**, 125, 054103; b) R. Improta, G. Scalmani, M. J. Frisch, V. Barone, *J. Chem. Phys.* **2007**, 127, 074504; c) P. Zhou, M. R. Hoffmann, K. Han, G. He, *J. Phys. Chem. B* **2014**, 119, 2125–2131.
- [24] B. Rkein, M. Manneveau, L. Noël-Duchesneau, K. Pasturaud, M. Durandetti, J. Legros, S. Lakhdar, I. Chataigner *Chem. Commun.* **2021**, 57, 10071–10074.
- [25] a) L. Goerigk, S. Grimme, *J. Chem. Phys.* **2010**, 132, 184103; b) D. Jacquemin, A. Planchat, C. Adamo, B. Mennucci, *J. Chem. Theory Comput.* **2012**, 8, 2359–2372; c) C. Fang, B. Oruganti, B. Durbjee, *J. Phys. Chem. A* **2014**, 118, 4157–4171.
- [26] A. D. Becke, *Phys. Rev. A* **1988**, 38, 3098–3100.
- [27] A. D. Becke, *J. Chem. Phys.* **1993**, 98, 5648–5652.
- [28] J. P. Perdew, *Phys. Rev. B* **1986**, 33, 8822–8824.
- [29] A. Austin, G. A. Petersson, M. J. Frisch, F. J. Dobek, G. Scalmani, K. Throssell, *J. Chem. Theory Comput.* **2012**, 8, 4989–5007.
- [30] Y. Zhao, D. G. Truhlar, *Theor. Chem. Acc.* **2008**, 120, 215–241.
- [31] R. Peverati, D. G. Truhlar, *Phys. Chem. Phys.* **2012**, 14, 16187–16191.
- [32] a) J. Heyd, G. E. Scuseria, *J. Chem. Phys.* **2004**, 121, 1187–1192; b) J. Heyd, G. E. Scuseria, *J. Chem. Phys.* **2004**, 120, 7274–7280; c) J. Heyd, J. E. Peralta, G. E. Scuseria, *J. Chem. Phys.* **2005**, 123, 174101; d) T. M. Henderson, A. F. Izmaylov, G. Scalmani, G. E. Scuseria, *J. Chem. Phys.* **2009**, 131, 044108.
- [33] T. M. Henderson, A. F. Izmaylov, G. E. Scuseria, A. Savin, *J. Chem. Theory Comput.* **2008**, 4, 1254–1262.
- [34] a) J. Tao, J. P. Perdew, V. N. Staroverov, G. E. Scuseria, *Phys. Rev. Lett.* **2003**, 91, 146401; b) V. N. Staroverov, G. E. Scuseria, *J. Chem. Phys.* **2003**, 119, 12129–12137.
- [35] A. D. Boese, N. C. Handy, *J. Chem. Phys.* **2002**, 116, 9559–9569.
- [36] T. Yanai, D. P. Tew, N. C. Handy, *Chem. Phys. Lett.* **2004**, 393, 51–57.
- [37] J.-D. Chai, M. Head-Gordon, *Phys. Chem. Chem. Phys.* **2008**, 10, 6615–6620.
- [38] a) H. Shi, J. Dai, X. Zhang, L. Xu, L. Wang, L. Shi, L. Fang, *Spectrochim. Acta. A. Mol. Biomol. Spectrosc.* **2011**, 83, 242–249; b) H. Chen, Y. Yan, N. Zhang, Z. Mo, Y. Xu, Y. Chen, *Org. Lett.* **2021**, 23, 376–381; c) K.-H. Lee, K. Morino, A. Sudo, T. Endo, *Polym. Bull.* **2011**, 67, 227–236; d) S. Dong, Z. Li, J. Qin, *J. Phys. Chem. B* **2009**, 113, 434–441; e) C. Han, Z. Zhang, H. Xu, S. Yue, J. Li, P. Yan, Z. Deng, Y. Zhao, P. Yan, S. Liu, *J. Am. Chem. Soc.* **2012**, 134, 19179–19188; f) P. A. St. John, J. L. Brook, R. H. Biggs, *Anal. Biochem.* **1967**, 18, 459–463; g) M. R. Hilaire, D. Mukherjee, T. Troxler, F. Gai, *Chem. Phys. Lett.* **2017**, 685, 133–138; h) M. Sun, P.-S. Song, *Photochem. Photobiol.* **1977**, 25, 3–9; i) M. Sayed, O. Younis, R. Hassanien, M. Ahmed, A. A. K. Mohammed, A. M. Kamal, O. Tsutsumi, *J. Photochem. Photobiol. C* **2019**, 383, 111969; j) S. Densil, C.-H. Chang, C.-L. Chen, A. Mathavan, A. Ramdass, V. Sathish, P. Thanasekaran, W.-S. Li, S. Rajagopal, *Luminescence* **2018**, 33, 780–789; k) J. Li, L. Zheng, L. Sun, C. Li, X. Zhang, S. Cheng, W. Hu, *J. Mater. Chem. C* **2018**, 6, 13257–13260; l) M. Johnsen, P. R. Ogilby, *J. Phys. Chem. A* **2008**, 112, 7831–7839; m) H. Ammar, *Dyes Pigm.* **2003**, 57, 259–265; n) M. E. M. Sakr, M. T. H. A. Kana, A. H. M. Elwahy, S. A. El-Daly, E.-Z. M. Ebeid, *J. Mol. Struct.* **2020**, 1206, 127690; o) Y. Li, T. Tan, S. Wang, Y. Xiao, X. Li, *Dyes Pigm.* **2017**, 144, 262–270.

Submitted: May 17, 2023

Accepted: June 20, 2023